Received: 27 January 2023 | Revised: 26 May 2023 | Accepted: 6 July 2023

DOI: 10.1002/prot.26557

RESEARCH ARTICLE

PROTEINS WILEY

Analysis of the crystal structure of a parallel three-stranded coiled coil

Matteo de March [1,2] | Neal Hickey [1] | Silvano Geremia [1]

[1]Department of Chemical and Pharmaceutical Sciences, University of Trieste, Trieste, Italy

[2]Laboratory for Environmental and Life Sciences, University of Nova Gorica, Nova Gorica, Slovenia

Correspondence
Matteo de March and Silvano Geremia, Department of Chemical and Pharmaceutical Sciences, University of Trieste, P. Europa 1, 34127, Trieste, Italy.
Email: matteo.demarch@ung.si; sgeremia@units.it

Funding information
CIRCMSB Bari

Abstract

Here, we present the crystal structure of the synthetic peptide KE1, which contains four K-coil heptads separated in the middle by the QFLMLMF heptad. The structure determination reveals the presence of a canonical parallel three stranded coiled coil. The geometric characteristics of this structure are compared with other coiled coils with the same topology. Furthermore, for this topology, the analysis of the propensity of the single amino acid to occupy a specific position in the heptad sequence is reported. A number of viral proteins use specialized coiled coil tail needles to inject their genetic material into the host cells. The simplicity and regularity of the coiled coil arrangement made it an attractive system for de novo design of key molecules in drug delivery systems, vaccines, and therapeutics.

KEYWORDS
crystal structure, geometry, heptad, parallel coiled coil, trimeric assembly

1 | INTRODUCTION

Seventy years ago, Crick and Pauling, during their preliminary exchange of views with successive correspondence on the disputed paternity of the coiled coil model of α-keratin (ropes with two or more α helical strands),[1] could not have imagined the importance of this protein architecture in nature. In fact, it is now recognized that coiled coils play relevant roles in oligomerization, DNA binding and gene regulation, ion transport, structural assembly, etc.[2,3] In recent years they have become even more prominent due to their replication role in viruses such as HIV[4] and SARS-Cov-2,[5,6] while they are increasingly used in biotechnological applications.[7–10] The first detailed description of the coiled coil assembly was reported in the seminal work of F.H.C. Crick,[11] in which the α-helices wrap around each other, with their side chains packed in a "knobs-into-holes" manner. The two-stranded coiled coil represents the most frequent oligomerization motif encountered in proteins.[12] However, trimeric,[13] tetrameric,[14] pentameric,[15] and hexameric[16] assemblies have been reported, for example, in viral proteins, while heptameric coiled coils have also been characterized.[17] The structural aspects of coiled coil assemblies have been extensively covered in the literature.[3,18] Briefly, the non-integral periodicity (3.63) of the ideal α-helix does not permit the side-by-side arrangement with undistorted α-helical strands. However, in the canonical coiled coil, left handed super-coiling of the α-helixes reduces the periodicity to 3.5 when viewed from the perspective of the bundle axis. Therefore, with regard to this super-helix axis the "knobs-into-holes" scheme is replicated every seven residues of each α-helix. The peptide sequence is characterized by repeated heptads with positions conventionally labeled *a*, *b*, *c*, *d*, *e*, *f*, and *g*. Generally, coiled coil structures of parallel amphipathic α-helices have a continuous nonpolar core formed by the side chains of hydrophobic residues located in the *a* and *d* positions; while the residues in positions *e* and *g*, which lie alongside this hydrophobic core, are typically charged residues involved in intra- or inter-helical salt bridge interactions.[19] The remaining positions (*b*, *c*, and *f*), located in the coiled coil surface exposed to the solvent, are generally occupied by hydrophilic residues. It is well known that there is a subtle mechanism that can select the formation of two, three or more stranded helixes, which is related

to the presence of specific buried hydrophobic residues at the *a* and *d* heptad positions.[20]

Significant research effort has been dedicated to the de novo design of peptides that are able to form homo or hetero coiled coils.[21–23] In particular, two sequences named K-coil (KVSALKE) and E-coil (EVSALEK) with complementary charges in positions *e*, *f*, and *g* of the heptad (the sequence starts with the residue in position *g* of the heptad for historical reasons) were designed for the formation of heterodimeric coiled coils.[24,25] In detail, the K_4 peptide, which consists of four copies of the K-coil heptad sequence, forms coiled-coil heterodimers with the complementary E_4 peptide, while the K_4 and E_4 peptides are random-coil on their own.[25,26] This opened the possibility of relevant biotechnological applications. For example, the peptide formed by five K-coil heptads, K_5 and its partner E_5 were used in multimerization of adenovirus serotype 3 fiber knob domains with potential application in the therapy of epithelial cancer and gene/drug delivery to normal epithelial tissues.[27] Recently, it has been shown that the K_5 peptide, when fused with proteins, functions as a cell penetrating peptide to enhance the intracellular delivery of proteins.[28] During our work with the synthetic peptide KE1, which contains four K-coil heptads separated in the middle by a phage-display selected sequence for xanthine recognition (QFLMLMF heptad), we have characterized, at atomic resolution, the X-ray structure of this peptide. Here, we present the details of the homotrimeric parallel coiled-coil structure observed for this peptide and its comparison with artificial and natural proteins in order to characterize the structural determinants which produce this specific coiled coil assembly.

2 | MATERIALS AND METHODS

KE1, kindly provided by Prof. F. Berti (University of Trieste), was synthesized using Fmoc/tBu solid-phase approach and purified by HPLC and its identity and MW (3993.7 Da) were later confirmed by Mass Spectrometry with ESI-IonTrap Esquire 4000 Bruker instrument.

Initial attempts to crystallize KE1 using the slow evaporation technique in various solvents, including EtOH 100%, EtOH:H_2O 50%:50%, TFE:H_2O 50%:50%, and TFE:EtOH 50%–50% did not yield any crystals. Subsequently, we employed a water solution of KE1 at a concentration of 3 mM (12 mg/ml) with theophylline 15 mM in vapor diffusion crystallization trials. The peptide concentration was estimated by Waddell's Method: $[C]_{mg/ml} = (A_{215} - A_{225}) * 144$. High throughput micro-crystallization trials were initially performed using Tecan Freedom Evo 100 in 96-well sitting drop crystallization plates. We screened conditions of PEG/Ion suite (Hampton), Classic, Classic II, and $AmSO_4$ suites (Qiagen). Most of the conditions produced roodlike shape crystals with orthorhombic cell ($Pna2_1$, $a = 24.6$ Å $b = 3.8$ Å $c = 8.5$ Å) which corresponded to the crystalline form of the pure theophylline. A second crystal form with pyramidal shape was observed in $(NH_4)_2SO_4$/PEG400 w/v based conditions. These crystals diffracted at very low resolution (7–9 Å). Using the stock protein solution without theophylline and optimizing the crystal conditions with the hanging-drop method, single pyramidal crystals grew within 7 days in 0.1 M NaHepes pH 7.5, 1.8–2.5 M $(NH_4)_2SO_4$ and 1.5–3% $PEG400_{w/v}$ to dimension of 0.4 * 0.2 mm. X-ray diffraction experiments were carried out at Elettra Synchrotron XRD1 beamline. Crystals were harvested into mother liquor supplemented by glycerol 30% and flash-frozen at 100 K. Diffraction data were collected at wavelength of 1.00 Å on a MARCCD (345_{mm}) image plate detector. Indexing, integration of reflection intensities and data scaling (Table S1) were performed using SCALA[29] from CCP4i.[30] The crystals[31] show a P321 crystallographic point group symmetry with unit cell axis *a*, $b = 22.36$ Å and $c = 51.01$ Å. The Matthew's coefficient[32] of 0.94 obtained with $Z = 6$ suggested merohedral twinning of P3 crystals, with one molecule in the asymmetric units (Table S1).

Molecular replacement method with AMoRE[33] was used to solve the structure of KE1 from twinned data starting from a 35 poly-alanine α-helical model. Merohedral twin[34] with twin fraction of 46% was solved using the twin law -k -h -l. In the first cycles of model building with Coot[35] and refinement with REFMAC5[36] the poly-Ala model was mutated following the KE1 sequence. Final twin refinement was conducted using SHELXL.[37] Final R_{work} and R_{free} values are reported in Table S1.

HeLANAL[38] was used to calculate the helical geometry of KE1. The same analysis was done for the structural homologs found in PDB, belonging to the most representative viral fusion coiled coils and predicted by DALI server[39] (Table S2). The list of trimeric coiled coil structures (Table S3) was obtained searching in the CC+ database for the parallel, homo-trimeric fold with sequence length > 28 residues.[40] The resulting assemblies were then analyzed with the CCCP (coiled coil crick parameterization) tool (Table 1)[41] and the distribution of the amino acids in the coiled coil positions was determined (Table 2). Pymol was used to prepare the figures.[42]

3 | RESULTS AND DISCUSSION

The crystal structure of KE1 (PDB code 3TQ2) was solved at near atomic resolution of 1.1 Å. Data reduction and refinement statistics are listed in Table S1. The asymmetric unit of the merohedrally twined trigonal (P3) crystals consists of one peptide chain, a sulfate ion, which forms a salt bridge interaction with Lys27 (2.73 Å), and 29 water molecules. The five heptads of KE1 fold as a single $\alpha 3.6_{13}$ helix (Figure 1A) with typical intra-helical hydrogen bonds. Interestingly, the central QFLMLMF heptad, selected for xanthine recognition, maintains the α-helix fold of the four K-coil heptads. This was unexpected because this heptad was selected for its binding abilities, rather than its helical propensity. In fact, based on the initial design,[43] we hoped that this region would adopt a loop structure for recognition of xanthine molecules between the aromatic aminoacyl residues, rather than a helical conformation. Therefore, we were surprised to find that the hydrophobic heptad inserted in this region led to the formation of a regular α-helix. This could be responsible for the poor and ambiguous results obtained in the recognition investigation of KE1. This fold is stabilized by an interaction between the side chains of Phe16 (position *a*) and Met20 (position *e*), already reported as a

TABLE 1 Crick parameters calculated with the CCCP tool for KE1 and for the 50 parallel trimeric coiled coil assemblies found in the CC+ database.

Crick parameters	KE1	Mean	Min	Max	ESD
Super-helical radius, R0 (Å)	6.50	6.37	5.56	6.64	0.19
Helical radius, R1 (Å)	2.27	2.26	1.90	2.32	0.06
Super-helical frequency, ω0 (°/res)	−3.4	−3.4	−4.0	−2.5	0.4
Helical frequency, ω1 (°/res)	102.9	102.9	101.8	106.2	0.6
Pitch angle, α (°)	−15.0	−14.3	−16.8	−10.8	1.5
Pitch (Å)	153	159	130	213	20
Rise per residue, d(Å)	1.512	1.509	1.496	1.567	0.011

TABLE 2 Frequency and distribution of the specific amino acids on the hydrophobic (*a*, *d*, grey), charged (*e*, *g*, green), and hydrophilic (*b*, *c*, *f*, yellow) coiled coil positions obtained from the 50 parallel trimeric coiled coil assemblies found in CC+ database.

	a	*b*	*c*	*d*	*e*	*f*	*g*
Ala	3.9%	14.3%	18.6%	8.1%	4.8%	7.6%	8.0%
Cys	1.2%	0.0%	0.0%	0.4%	0.0%	0.0%	0.0%
Asp	0.8%	10.0%	10.5%	0.7%	7.2%	6.4%	8.8%
Glu	0.8%	8.8%	15.8%	1.1%	25.5%	11.6%	14.4%
Phe	1.5%	0.4%	0.4%	1.1%	0.4%	0.8%	0.0%
Gly	0.8%	3.2%	2.0%	0.0%	4.4%	8.0%	0.8%
His	1.2%	0.4%	2.4%	4.4%	0.8%	0.0%	1.2%
Ile	30.9%	1.6%	0.4%	18.5%	0.8%	2.0%	0.4%
Lys	1.5%	7.6%	4.9%	0.4%	10.4%	10.8%	12.4%
Leu	21.6%	2.8%	4.5%	34.4%	5.6%	2.4%	5.2%
Met	1.5%	0.4%	0.8%	2.6%	1.2%	0.4%	1.6%
Asn	2.3%	6.8%	2.4%	10.0%	5.6%	6.4%	5.2%
Pro	0.0%	0.0%	0.4%	0.0%	0.0%	0.4%	0.0%
Gln	4.6%	8.0%	10.9%	5.6%	11.2%	12.4%	7.6%
Arg	0.8%	6.8%	5.3%	1.1%	5.2%	6.0%	20.8%
Ser	1.2%	13.1%	8.5%	1.5%	6.8%	10.0%	6.0%
Thr	1.9%	9.6%	8.9%	2.2%	7.6%	8.8%	5.6%
Val	23.2%	3.6%	2.8%	7.8%	2.0%	5.2%	2.0%
Trp	0.0%	0.0%	0.0%	0.0%	0.0%	0.0%	0.0%
Tyr	0.4%	2.8%	0.4%	0.0%	0.8%	0.4%	0.0%
	Ile	Ala	Ala	Leu	Glu	Gln	Arg

stabilizing factor of an α–helical peptide via shared rotamer preferences.[44] The helix geometry, calculated by HELANAL,[38] is curved, with an average and maximum bending angles of 5.1° and 17.2°, respectively, and with a curvature radius of 85 Å (rmsd = 0.11 Å). Curved helices are more abundant in natural protein with respect to the kinked helices and the even more rare linear helices.[38] The curvature of the helices is important for the efficient knobs-into-hole packing of helices and it allows the sequestration into the hydrophobic core of both anions[45] and cations.[46] The importance of flexibility and adaptability of helices has been recognized in metal-assisted stabilization of collagenous triple helices[47] and metal-dependent catalytic activity in designed three-stranded coiled coils.[48] Flexibility is clearly an advantage for viral fusion domains during the transition from pre- to post-fusion arrangement. In fact, class I viruses use the α-helix-rich domains to fuse their membrane to the host-cell membrane and deliver the viral genome into the host cytoplasm for replication.[49] For instance, SARS-Cov-2 Spike pre-fusion protein undergoes a conformational change triggered by a cleavage event at the cell surface that generates the post-fusion arrangement.[50] Similarly, the HIV inactive gp41-gp120 domain becomes active when the core of gp41 folds as a coiled coil.[51] An analysis of the KE1 helix deformation in comparison with some of the most representative structural homologs found in PDB with DALI server and belonging to viral fusion proteins is reported in Table S2.

The crystallographic threefold axes observed in the crystal structure of KE1 produce a quaternary structure characterized by parallel three-stranded coiled coils (Figure 1B). Positions *a* in the trimeric assembly of the K-coil heptads are occupied by valines, whose side chains interact in the hydrophobic core. On the contrary, in the central heptads the same positions are occupied by Phe16 residues, whose aromatic groups point toward the external surface. The second heptad positions, *d*, crucial for the formation of the hydrophobic core, are occupied in all five heptads by leucine residues whose side chains are tightly packed. Positions *e* and *g* are occupied by Lys residues in the K-coil heptads, while the central heptads have Met20 and Gln15 residues, respectively (Figure 1B). Due to the trigonal symmetry and cell translation, KE1 assembles as a super-helix which develops along the c axis, with the C-terminal of one helix adjacent to the N-terminal of the equivalent helix generated by the threefold rotation and cell translation to form a pseudo-continuous α-helix (Figure 1C). Therefore, the super-helix has a periodicity of about 150 Å, which corresponds to the three times the *c* axis dimension. Each single-peptide wraps around the axis of the super-helix by 120° with a contribution from each single heptad of 24°. Although sterically and electrostatically unfavored with respect to the antiparallel fold,[52,53] parallel coiled coils are found in many natural and artificial proteins.[3] For example, a similar crystallographic arrangement was observed for the coil-V_aL_d, a 29-residue designed trimeric coiled coil,[54] while a three helix parallel coiled coil arrangement has been described for the phage P22 cell envelope-penetrating tail needle gp26[55] (Figure 1D). Moreover, for its similarity to the class I fusion peptides, this specific arrangement has acquired importance in biomedicine. An example is given by the use of N3G mimicking the inner core post fusion gp41, designated as promising therapeutic against HIV infection.[56] This peptide was also highly effective in inhibiting infection of human β-coronaviruses

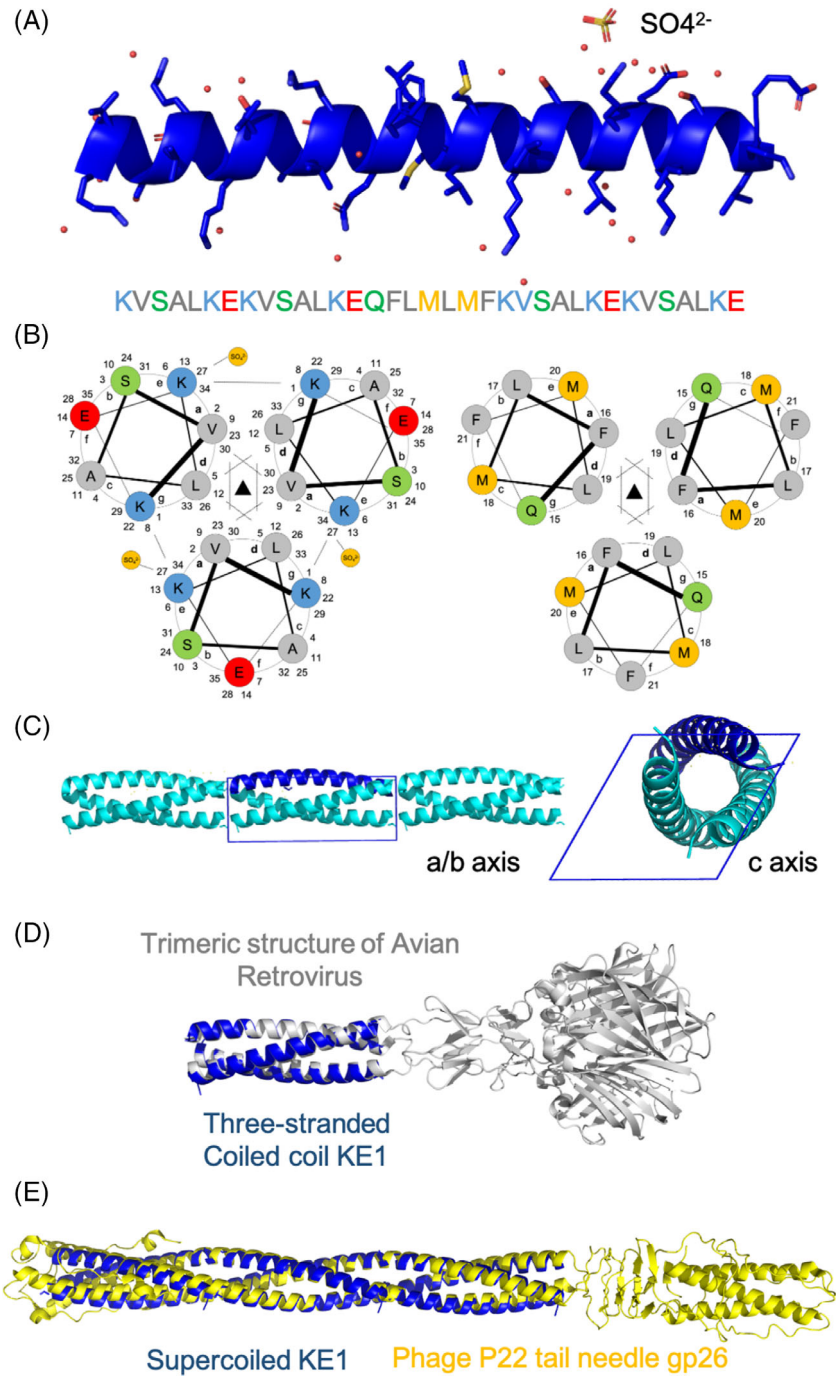

FIGURE 1 Experimental crystal structure of KE1. (A) The helix $\alpha 3.6_{13}$ is shown with the sulfate ion and water molecules. The sequence is indicated at the bottom where positively charged residues are highlighted in blue, negatively charged in red, polar in green, apolar in gray and methionine in yellow. (B) Packing of the three stranded coiled coil KE1 with the two heptads KVSALKE (left) and QFLMLMF (right). Color code is the same as in A. (C) The supercoil crystal structure of KE1 along *a/b* and *c* axes. (D) Superposition of KE1 to the structure of Avian Retrovirus fusion domain (PDB 2JJL). (E) Superposition of the supercoiled KE1 to the trimeric structure of the Phage 22 tail needle gp26 (PDB 3C9I).

possibly by binding the HR2 region in the spike protein to block their hexameric structure formation.[56] The KE1 arrangement is remarkably similar to the fusion domain of the Avian Retrovirus[13] (Figure 1E). The two structures overlap with a RMSD value of 0.98 Å.

With respect to other coiled coils, the parallel trimeric arrangement is less frequent in nature. 50 parallel trimeric coiled coil structures with sequence length > 28 residues found in the CC+ database[40] were analyzed for a comparison with KE1 (Table S3). Most of these structures belong to viral domains, but ion channel and structural protein domains are also represented. For these structures the mean, maximum, minimum and ESD values of the Crick's parameters calculated using CCCP[41] are reported in Table 1. The super-helical and helical radii (R0, R1), the super-helical and helical frequency (ω0, ω1), the pitch height and angle (α), and the rise per residue (d) of KE1 are very close to the mean values here reported. The mean R0 value extracted from our analysis is 6.37 Å, very closed to 6.50 Å for KE1. The mean value of ω0 (°/res) and α are −3.4° and − 14.3° compared and KE1 values of −3.4° and −15.0°, respectively. The distribution of each amino acid on the hydrophobic (*a*, *d*, gray), hydrophilic (*e*, *g*, green) and neutral (*b*, *c*, *f*, yellow) positions considering all the sequences of the selected parallel trimeric coiled coils is shown in Table 2. Those residues with abundance >10% are highlighted and

among these the most frequently encountered are enclosed in a black outline. Not surprisingly, Ile (30.9%) and Leu (34.4%) lie on hydrophobic positions *a* and *d*, while Glu (25.5%) and Arg (20.8) are found in positions *e* and *g*, where charged residues are typically involved in intra- or inter-helical salt bridge interactions. The other positions, located in the coiled coil surface exposed to the solvent, show more variation in terms of residues present. The Ala residue prevails in positions *b* (14.3%) and *c* (18.6%) while the hydrophilic residue Gln is the most frequent at the *f* position (12.4%).

The original K_4 peptide is known, from CD spectra, to be random-coil on its own, while it can fold into a stable coiled-coil structure when paired with the complementary E_4 peptide.[25,26] To the best of our knowledge, there is no direct evidence reported in literature that addition of a further K-coil heptad produces in the K_5 peptide a coiled coil structure. The only crystal structure deposited in Protein Data Bank containing the K-coil sequence is a fusion of K_5 peptide to a mutant adenovirus 3 knob domain (4LIY).[57] However, even if the observed homotrimeric assembly of the viral protein could be compatible with the homotrimeric coiled coil of the K_5 domain, this portion of the structure was not modeled in the electron density maps because completely disordered. On the other hand, previous studies of K-coil and E-coil variants show that increasing the number of heptad repeats promotes in the single peptide the coiled coil formation.[25] For example, it was observed that the single peptide VAAL-K_3 assumes a random coil structure, while with a further heptad, the VAAL-K_4 peptide assumes a coiled-coil structure. Therefore, the introduction of the central hydrophobic heptad seems crucial for the formation of the coiled coil motif in KE1 for two main reasons: for the elongation of the α-helical peptide, passing from 4 to 5 heptads, or for a hypothetical triggering role of the coiled-coil structure due to its specific sequence. With regard to the triggering of the coiled-coil formation, there are two main proposals: one with the initial formation of helixes and then the formation of the coiled-coil (in this case the propensity of formation of alpha helix is the crucial point) and one with the formation of nucleation sites outside the region with high helix propensity, which region is the last to fold (in this case the formation of a hydrophobic core is the crucial point).[2] Therefore, the hydrophobic heptad inserted into the central region of KE1 could in fact be responsible for driving the formation of the trimeric coiled-coil structure observed in our study. However, the precise mechanism by which the hydrophobic heptad induces the formation of the trimeric coiled-coil structure is quite complicated and likely involves a combination of hydrophobic interactions, steric effects, and changes in the helical register of the flanking K-coil heptads.

4 | CONCLUSION

Here, we have described the structure of the new synthetic peptide KE1, designed with four K-coil heptads separated in the middle by a phage-display selected sequence for xanthine recognition. Unexpectedly, the central heptad also adopted a regular helical structure, despite the presence in the sequence of residues, such as Phe, with more propensity to participate in β-strand than α-helical secondary structures. The crystallographic parallel trimeric coiled coil arrangement has been compared with the other parallel trimeric coiled coils structures reported in the CC+ database. The analysis of the residue distribution specific for each heptad positions at the basis of this critical assembly gives an additional description to implement the previous knowledge about parallel three stranded coiled coils.

AUTHOR CONTRIBUTIONS

Matteo De March: Investigation; writing – original draft; writing – review and editing; methodology; formal analysis. **Neal Hickey:** Writing – review and editing; data curation. **Silvano Geremia:** Conceptualization; funding acquisition; writing – review and editing; supervision; methodology.

ACKNOWLEDGMENT

We thank Prof. F. Berti for the chemical synthesis.

CONFLICT OF INTEREST STATEMENT

The authors have declared no conflict of interest.

PEER REVIEW

The peer review history for this article is available at https://www.webofscience.com/api/gateway/wos/peer-review/10.1002/prot.26557.

DATA AVAILABILITY STATEMENT

All data supporting this study can be requested to the corresponding authors.

ORCID

Matteo de March https://orcid.org/0000-0002-3447-957X
Silvano Geremia https://orcid.org/0000-0002-0711-5113

REFERENCES

1. Gruber M, Lupas AN. Historical review: another 50th anniversary: new periodicities in coiled coils. *Trends Biochem Sci*. 2003;28:679-685. doi:10.1016/j.tibs.2003.10.008
2. Mason JM, Arndt KM. Coiled coil domains: stability, specificity, and biological implications. *Chembiochem*. 2004;5:170-176. doi:10.1002/cbic.200300781
3. Lupas AN, Bassler J. Coiled coils: a model system for the 21st century. *Trends Biochem Sci*. 2017;42:130-140. doi:10.1016/j.tibs.2016.10.007
4. Skehel JJ, Wiley DC. Coiled coils in both intracellular vesicle and viral membrane fusion. *Cell*. 1998;95:871-874. doi:10.1016/S0092-8674(00)81710-9
5. Jackson CB, Farzan M, Chen B, Choe H. Mechanisms of SARS-CoV-2 entry into cells. *Nat. Rev. Mol. Cell Biol*. 2022;23:3-20. doi:10.1038/s41580-021-00418-x
6. Zheng Q, Deng Y, Liu J, van der Hoek L, Berkhout B, Lu M. Core structure of S2 from the human coronavirus NL63 spike glycoprotein. *Biochemistry*. 2006;45:15205-15215. doi:10.1021/bi061686w
7. Berwick MR, Lewis DJ, Jones AW, et al. Novo design of In(III) coiled coils for imaging applications. *J Am Chem Soc*. 2014;136:1166-1169. doi:10.1021/ja408741h
8. Utterström J, Naeimipour S, Selegård R, Aili D. Coiled coil-based therapeutics and drug delivery systems. *Adv Drug Deliv Rev*. 2021;170:26-43. doi:10.1016/j.addr.2020.12.012

9. Wu Y, Collier JH. α-Helical coiled-coil peptide materials for biomedical applications. *WIREs Nanomed Nanobiotechnol*. 2017;9:1-33. doi:10.1002/wnan.1424
10. Outlaw VK, Bottom-Tanzer S, Kreitler DF, Gellman SH, Porotto M, Moscona A. Dual inhibition of human parainfluenza type 3 and respiratory syncytial virus infectivity with a single agent. *J Am Chem Soc*. 2019;141:12648-12656. doi:10.1021/jacs.9b04615
11. Crick FHC. The packing of α-helices: simple coiled-coils. *Acta Crystallogr*. 1953;6:689-697. doi:10.1107/s0365110x53001964
12. Burkhard P, Kammerer RA, Steinmetz MO, Bourenkov GP, Aebi U. The coiled-coil trigger site of the rod domain of Cortexillin I unveils a distinct network of interhelical and intrahelical salt bridges. *Structure*. 2000;8:223-230. doi:10.1016/S0969-2126(00)00100-3
13. Guardado-Calvo P, Fox GC, Llamas-Saiz AL, van Raaij MJ. Crystallographic structure of the α-helical triple coiled-coil domain of avian reovirus S1133 fibre. *J Gen Virol*. 2009;90:672-677. doi:10.1099/vir.0.008276-0
14. Tarbouriech N, Curran J, Ruigrok RWH, Burmeister WP. Tetrameric coiled coil domain of Sendai virus phosphoprotein. *Nat Struct Biol*. 2000;7:777-781. doi:10.1038/79013
15. Chacko AR, Arifullah M, Sastri NP, et al. Novel pentameric structure of the diarrhea-inducing region of the rotavirus enterotoxigenic protein NSP4. *J Virol*. 2011;85:12721-12732. doi:10.1128/jvi.00349-11
16. Chan DC, Fass D, Berger JM, Kim PS. Core structure of Gp41 from the HIV envelope glycoprotein. *Cell*. 1997;89:263-273. doi:10.1016/S0092-8674(00)80205-6
17. Liu J, Zheng Q, Deng Y, Cheng CS, Kallenbach NR, Lu M. A seven-helix coiled coil. *Proc Natl Acad Sci U S A*. 2006;103:15457-15462. doi:10.1073/pnas.0604871103
18. Truebestein L, Leonard TA. Coiled-coils: the long and short of it. *Bioessays*. 2016;38:903-916. doi:10.1002/bies.201600062
19. Kohn WD, Kay CM, Hodges RS. Salt effects on protein stability: two-stranded α-helical coiled-coils containing inter- or intrahelical ion pairs. *J Mol Biol*. 1997;267:1039-1052. doi:10.1006/jmbi.1997.0930
20. Harbury PB, Zhang T, Kim PS, Alber T. A switch between two-, three-, and four-stranded coiled coils in GCN4 leucine zipper mutants. *Science (80−)*. 1993;262:1401-1407. doi:10.1126/science.8248779
21. Lapenta F, Aupič J, Strmšek Ž, Jerala R. Coiled coil protein origami: from modular design principles towards biotechnological applications. *Chem Soc Rev*. 2018;47:3530-3542. doi:10.1039/c7cs00822h
22. Rink WM, de Thomas F. Novo designed α-helical coiled-coil peptides as scaffolds for chemical reactions. *Chem: A Eur J*. 2019;25:1665-1677. doi:10.1002/chem.201802849
23. Boyken SE, Benhaim MA, Busch F, et al. De novo design of tunable, PH-driven conformational changes. *Science (80−)*. 2019;364:658-664. doi:10.1126/science.aav7897
24. Tripet B, Yu L, Bautista DL, Wong WY, Irvin RT, Hodges RS. Engineering a de novo designed coiled-coil heterodimerization domain for the rapid detection, purification and characterization of recombinantly expressed peptides and proteins (protein engineering [1996] 9 [1029-1042]). *Protein Eng*. 1997;10:299.
25. Litowski JR, Hodges RS. Designing heterodimeric two-stranded α-helical coiled-coils. Effects of hydrophobicity and α-helical propensity on protein folding, stability, and specificity. *J Biol Chem*. 2002;277:37272-37279. doi:10.1074/jbc.M204257200
26. Aronsson C, Dånmark S, Zhou F, et al. Self-sorting heterodimeric coiled coil peptides with defined and tuneable self-assembly properties. *Sci Rep*. 2015;5:1-10. doi:10.1038/srep14063
27. Wang H, Li Z, Yumul R, et al. Multimerization of adenovirus serotype 3 fiber knob domains is required for efficient binding of virus to Desmoglein 2 and subsequent opening of epithelial junctions. *J Virol*. 2011;85:6390-6402. doi:10.1128/jvi.00514-11
28. Li J, Tuma J, Han H, et al. The coiled-coil forming peptide (KVSALKE) 5 is a cell penetrating peptide that enhances the intracellular delivery of proteins. *Adv Healthc Mater*. 2022;11:1-12. doi:10.1002/adhm.202102118
29. Evans P. Scaling and assessment of data quality. *Acta Crystallogr Sect D Biol Crystallogr*. 2006;62:72-82. doi:10.1107/S0907444905036693
30. Project C.C. The CCP4 suite: programs for protein crystallography. *Acta Crystallogr. Sect. D Biol. Crystallogr*. 1994;50:760-763. doi:10.1107/S0907444994003112
31. Helliwell JR. Macromolecular crystal twinning, lattice disorders and multiple crystals. *Crystallogr Rev*. 2008;14:189-250.
32. Matthews BW. Solvent content of protein crystals. *J Mol Biol*. 1968;33:491-497. doi:10.1016/0022-2836(68)90205-2
33. Navaza J. AMoRe: an automated package for molecular replacement. *Acta Crystallogr Sect A*. 1994;50:157-163. doi:10.1107/S0108767393007597
34. Yeates TO. Detecting and overcoming crystal twinning. *Methods Enzymol*. 1997;276:344-358. doi:10.1016/S0076-6879(97)76068-3
35. Emsley P, Lohkamp B, Scott WG, Cowtan K. Features and development of coot. *Acta Crystallogr. Sect. D Biol. Crystallogr*. 2010;66:486-501. doi:10.1107/S0907444910007493
36. Murshudov GN, Vagin AA, Dodson EJ. Refinement of macromolecular structures by the maximum-likelihood method. *Acta Crystallogr. Sect. D Biol. Crystallogr*. 1997;53:240-255. doi:10.1107/S0907444996012255
37. Sheldrick GM. A short history of SHELX. *Acta Crystallogr Sect A Found Crystallogr*. 2008;64:112-122.
38. Kumar P, Bansal M. HELANAL-plus: a web server for analysis of helix geometry in protein structures. *J Biomol Struct Dyn*. 2012;30:773-783. doi:10.1080/07391102.2012.689705
39. Holm L, Rosenström P. Dali server: conservation mapping in 3D. *Nucleic Acids Res*. 2010;38:545-549. doi:10.1093/nar/gkq366
40. Testa OD, Moutevelis E, Woolfson DN. CC+: a relational database of coiled-coil structures. *Nucleic Acids Res*. 2009;37:315-322. doi:10.1093/nar/gkn675
41. Grigoryan G, Degrado WF. Probing designability via a generalized model of helical bundle geometry. *J Mol Biol*. 2011;405:1079-1100. doi:10.1016/j.jmb.2010.08.058
42. DeLano WL. The case for open-source software in drug discovery. *Drug Discov Today*. 2005;10:213-217. doi:10.1016/S1359-6446(04)03363-X
43. Pavan S, Berti F. Short peptides as biosensor transducers. *Anal Bioanal Chem*. 2012;402:3055-3070. doi:10.1007/s00216-011-5589-8
44. Iqbalsyah TM, Doig AJ. Pairwise coupling in an Arg-Phe-met triplet stabilizes α-helical peptide via shared rotamer preferences. *J Am Chem Soc*. 2005;127:5002-5003. doi:10.1021/ja043446e
45. Hartmann MD, Ridderbusch O, Zeth K, et al. A coiled-coil motif that sequesters ions to the hydrophobic core. *Proc Natl Acad Sci U S A*. 2009;106:16950-16955. doi:10.1073/pnas.0907256106
46. Geremia S, di Costanzo L, Randaccio L, et al. Response of a designed metalloprotein to changes in metal ion coordination, exogenous ligands, and active site volume determined by X-ray crystallography. *J Am Chem Soc*. 2005;127:17266-17276. doi:10.1021/ja054199x
47. Koide T, Yuguchi M, Kawakita M, Konno H. Metal-assisted stabilization and probing of collagenous triple helices. *J Am Chem Soc*. 2002;124:9388-9389. doi:10.1021/ja026182+
48. Pinter TBJ, Manickas EC, Tolbert AE, et al. Making or breaking metal-dependent catalytic activity: the role of stammers in designed three-stranded coiled coils. *Angew Chem Int Ed*. 2020;59:20445-20449. doi:10.1002/anie.202008356
49. Podbilewicz B. Virus and cell fusion mechanisms. *Annu Rev Cell Dev Biol*. 2014;30:111-139. doi:10.1146/annurev-cellbio-101512-122422
50. Xia X. Domains and functions of spike protein in Sars-Cov-2 in the context of vaccine design. *Viruses*. 2021;13:1-16. doi:10.3390/v13010109

51. Mao Y, Wang L, Gu C, et al. Subunit organization of the membrane-bound HIV-1 envelope glycoprotein trimer. *Nat Struct Mol Biol*. 2012;19:893-899. doi:10.1038/nsmb.2351
52. Oakley MG, Hollenbeck JJ. The design of antiparallel coiled coils. *Curr Opin Struct Biol*. 2001;11:450-457. doi:10.1016/s0959-440x(00)00232-3
53. Gurnon DG, Whitaker JA, Oakley MG. Design and characterization of a homodimeric antiparallel coiled coil. *J Am Chem Soc*. 2003;125:7518-7519. doi:10.1021/ja0357590
54. Ogihara NL, Weiss MS, Degrado WF, Eisenberg D. The crystal structure of the designed trimeric coiled coil coil- V(a)L(d): implications for engineering crystals and supramolecular assemblies. *Protein Sci*. 1997;6:80-88. doi:10.1002/pro.5560060109
55. Olia AS, Casjens S, Cingolani G. Structure of phage P22 cell envelope-penetrating needle. *Nat Struct Mol Biol*. 2007;14:1221-1226. doi:10.1038/nsmb1317
56. Wang C, Xia S, Wang X, et al. Supercoiling structure-based design of a trimeric coiled-coil peptide with high potency against HIV-1 and human β-coronavirus infection. *J Med Chem*. 2022;65:2809-2819. doi:10.1021/acs.jmedchem.1c00258
57. Wang H, Yumul R, Cao H, et al. Structural and functional studies on the interaction of adenovirus fiber knobs and desmoglein 2. *J Virol*. 2013;87:11346-11362. doi:10.1128/jvi.01825-13

SUPPORTING INFORMATION

Additional supporting information can be found online in the Supporting Information section at the end of this article.

How to cite this article: de March M, Hickey N, Geremia S. Analysis of the crystal structure of a parallel three-stranded coiled coil. *Proteins*. 2023;91(9):1254-1260. doi:10.1002/prot.26557